Discover Oncology

RESEARCH Open Access

Integrated single-cell and functional analyses define strategies to enhance dendritic cell immunostimulatory capacity

Yuting Li[1,2†], Huanhuan Li[3†], Chao Li[1], Rongrui Liu[2], Sisi Ye[2], Juan Li[2], Chuanhua Zhao[2], Xiaomin Ma[3], Xudong Cheng[3*] and Jianming Xu[2*]

[†]Yuting Li and Huanhuan Li contributed equally to this work.

*Correspondence:
Xudong Cheng
Chengxudong@zskybio.com
Jianming Xu
jmxu2003@163.com
[1]Department of Oncology, The First Medical Center, Chinese PLA General Hospital/Medical School of Chinese PLA, Beijing, China
[2]Senior Department of Oncology, Chinese PLA General Hospital, Beijing, China
[3]ZSky BioTech Co. LTD, Beijing, China

Abstract

Dendritic cells (DCs) are essential for the initiation and regulation of antitumor immune responses. Although DC vaccines hold great promise in personalized cancer immunotherapy, their efficacy remains limited by tumor-induced immunosuppression and insufficient DC maturation and activation. Recent studies suggest that DC maturation is accompanied by dynamic changes in immune checkpoint signaling, highlighting the need to better define functional DC states. To delineate these regulatory features, we performed single-cell RNA sequencing to characterize DC heterogeneity and transcriptional programs, identifying enrichment of immune checkpoint associated signatures, including PD-L1, within mature DC subsets. Subsequently, we evaluated the effects of PD-L1 blockade and CD40 stimulation on DC activation and function in vitro. We found that combined PD-L1 inhibition and CD40 engagement enhanced DC maturation and antigen-presenting capacity. We operationally define these functionally optimized DCs as "Enhanced DCs", characterized by elevated IL-12 secretion, and improved T-cell priming efficiency. When loaded with tumor neoantigen peptides, Enhanced DCs effectively activated $CD8^+$ T cells and promoted memory T-cell differentiation in co-culture assays. Together, this study integrates single-cell transcriptomic profiling with functional validation to demonstrate that targeted modulation of DC immune checkpoints and co-stimulatory pathways can improve the immunogenicity of DC, particularly when loaded with neoantigens. These findings provide a rational framework for optimizing DC-based cancer vaccines and advancing personalized immunotherapy approaches.

Keywords Single-cell genomics, Dendritic cell vaccine, PD-L1 antibody, CD40 agonist, Neoantigen, Cancer immunotherapy

1 Introduction

Dendritic cells (DCs) are the most potent professional antigen-presenting cells (APCs) that bridge innate and adaptive immunity, maintain immune tolerance, and initiate antigen-specific immune responses [1]. Activated DCs capture and process tumor antigens and present them to naïve T cells via major histocompatibility complex (MHC)

molecules while upregulating costimulatory molecules (CD80, CD86), promoting T-cell differentiation into effector cells and establishing tumor-specific immunity. DCs also secrete cytokines such as interleukin-12 (IL-12) to regulate T-cell activation, differentiation, and migration, contributing to durable antitumor immune responses [2]. Therefore, DCs are an ideal platform for therapeutic cancer vaccines [3–5].

Although DC vaccines have shown safety and immunogenicity in early clinical trials, their efficacy remains limited due to insufficient DC maturation and tumor-associated immunosuppression [6, 7]. Neoantigens, derived from tumor-specific mutations absent in normal tissues, are highly immunogenic and capable of inducing potent and durable antitumor immunity [8, 9]. However, the efficacy of neoantigen vaccines depends largely on efficient DC uptake, processing, and presentation. The immature or tolerogenic DCs are insufficient to elicit strong T-cell responses, limiting clinical translation. Enhancing DC maturation and function is therefore critical for improving immunotherapy efficacy.

In recent years, advances in single-cell genomics have provided powerful tools to dissect immune cell heterogeneity and functional states. Single-cell RNA sequencing (scRNA-seq) enables systematic profiling of DC composition, differentiation trajectories, and functional programs at single-cell resolution, thereby uncovering regulatory features that are often obscured in bulk analyses. Accumulating evidence indicates that tumor-associated DCs comprise heterogeneous populations with distinct maturation states and immunoregulatory features. Notably, some mature DC subsets acquire strong antigen-presenting capacity while simultaneously upregulating immune checkpoint molecules, which may constrain their ability to effectively prime T cells.

Previous studies have shown that PD-L1 blockade not only inhibits the PD-1/PD-L1 pathway but can also restore DC function by interrupting the PD-L1/B7.1 inhibitory signal on DCs [10, 11]. In addition, CD40, an important costimulatory molecule expressed on the surface of DCs, plays a critical role in regulating their maturation and function. CD40/CD40L interaction promotes DC maturation, upregulates MHC and costimulatory molecules, and induces IL-12 secretion, thereby enhancing T-cell activation [12, 13]. This dual effect promotes T-cell priming and activation while improving T-cell infiltration and effector function within the tumor microenvironment [11, 14]. However, systematic studies investigating the combined effects of PD-L1 blockade and CD40 stimulation to optimize DC vaccines are lacking.

Here, we first applied single-cell transcriptomic analysis to systematically characterize DC heterogeneity and functional states, with a particular focus on immunoregulatory signaling in mature DC subsets. Subsequently, we combined PD-L1 blockade and CD40 stimulation to generate functionally optimized DCs, hereafter termed “Enhanced DCs” defined by coordinated upregulation of maturation markers, increased cytokine production, and improved T-cell priming efficiency. We further loaded these Enhanced DCs with tumor neoantigen peptides (Neo-DCs) and evaluated their capacity to induce T-cell activation and memory differentiation in vitro. This strategy offers insights into the design of next-generation personalized immunotherapies targeting neoantigens.

2 Materials and methods

2.1 Data acquisition and preprocessing

Single-cell RNA sequencing (scRNA-seq) data were obtained from the Gene Expression Omnibus (GEO) database under accession number GSE189357 (https://www.ncbi

.nlm.nih.gov/geo/), which includes tumor samples from nine patients with primary lung adenocarcinoma (LUAD). Raw gene-cell expression matrices were processed in R (version 4.4.1). Quality control was performed to remove low-quality cells and genes. Genes expressed in fewer than five cells were excluded. Cells were retained if they met the following criteria: detection of 400–7,000 genes per cell, mitochondrial gene content < 10%, and erythrocyte-related gene expression < 3% (including HBB, HBA1, and HBA2). After filtering, 111,595 high-quality cells were retained for downstream analyses. To minimize batch effects across samples from different patients, normalized expression data were integrated using the Harmony algorithm. The corrected expression matrix was subsequently used for dimensionality reduction, clustering, and downstream functional analyses.

2.2 Single-cell transcriptomic analysis

Single-cell analyses were performed using the Seurat package (version 4.4.0). Following data normalization and scaling, highly variable genes were identified, and principal component analysis (PCA) was conducted for dimensionality reduction. The top principal components were selected based on elbow plots and variance explained. Cell clustering was performed using the FindNeighbors and FindClusters functions with a resolution of 0.5. Uniform Manifold Approximation and Projection (UMAP) was used for two-dimensional visualization of cell clusters. Differentially expressed genes (DEGs) for each cluster were identified using the FindAllMarkers function, with an adjusted p value < 0.05 and |log2 fold change| > 0.25. Cell clusters were annotated based on canonical marker genes for major LUAD cell types, including epithelial cells, endothelial cells, lymphoid cells, and myeloid populations. Myeloid cells were further subsetted and re-analyzed following the same pipeline to resolve finer cellular heterogeneity. DC subsets were identified and classified according to established marker genes for plasmacytoid DCs (pDCs), conventional DC1 (cDC1), conventional DC2 (cDC2), and LAMP3^{+} conventional DC3 (cDC3).

2.3 Cell–cell communication and gene enrichment analyses

Intercellular communication among myeloid cell subsets was inferred using the CellChat R package. Ligand-receptor interactions were analyzed based on curated signaling pathways, and the number and strength of interactions between different cell populations were quantified. Communication networks were visualized to highlight dominant signaling interactions among DCs, monocytes, and macrophage subsets. To characterize functional differences among DC subsets, pathway activity was evaluated using single-sample gene set enrichment analysis (ssGSEA). Hallmark gene sets and curated immune-related pathways were used to calculate enrichment scores for individual cells, which were then compared across DC subsets to identify distinct activation, migration, immune regulation, and metabolic states. In addition, transcription factor regulatory activity was assessed using the SCENIC pipeline (version 1.3.1). Regulons were defined as transcription factors and their target genes, and regulon activity scores were calculated for each cell. Differences in regulon activity among DC subsets were used to infer distinct transcriptional regulatory programs underlying DC functional states.

2.4 Human DC isolation and culture

No established cell lines were used in this study. Dendritic cells and $CD8^+$ T cells were generated from peripheral blood mononuclear cells (PBMCs) isolated from healthy adult donors.

Peripheral blood was collected from healthy donors with ethics committee approval and written informed consent. PBMCs were isolated by Ficoll-Paque (GE Healthcare) density gradient centrifugation (400 × g, 30 min, room temperature). $CD14^+$ monocytes were then purified using CD14 nanobeads (Miltenyi Biotec) and seeded at $1.5–2.5 \times 10^6$ cells/mL in serum-free DC medium (CellGenix) supplemented with recombinant human GM-CSF (50 ng/mL, R&D Systems) and IL-4 (20 ng/mL, R&D Systems). Cells were cultured at 37 °C in 5% CO_2 for 6 days, with medium replacement and cytokine supplementation on day 3. On day 6, immature DCs (imDCs) were harvested and loaded with antigen peptides as indicated. To induce maturation, cells were cultured in medium containing GM-CSF, IL-4, TNF-α (10 ng/mL), IL-1β (2 ng/mL), IL-6 (10 ng/mL), PGE_2 (1 μg/mL), and poly I: C (10 μg/mL) for 16–20 h. CD40 antibody (1 μg/mL) and/or PD-L1 antibody (10 μg/mL) were added 1–3 h before harvesting. Matured DCs (mDC) were then washed and collected for downstream experiments.

2.5 Neoantigen peptide identification and generation of Neo-DCs

Previous studies have shown that the p53 R175H mutation in the KLE cell line generates the neoantigen $p53^{R175H}$ (HMTEVVRHC) [15, 16]. After Sanger sequencing verification, a 21-mer peptide spanning this mutation (QSQHMTEVVRHCPHHERCSDS) was synthesized as $p53^{R175H}$ peptide.

DCs were prepared as described above. On day 6, the culture medium was replaced with serum-free DC medium containing the synthetic $p53^{R175H}$ peptide and maturation factors, and cells were incubated at 37 °C, 5% CO_2 for 20 h. Three hours prior to harvesting, PD-L1 antibody Atezolizumab (10 μg/mL, Roche) and CD40 antibody Cifurtilimab (1 μg/mL, MCE) were added. Cells were washed and harvested to obtain neoantigen-loaded mature DCs (Neo-DCs).

2.6 Cell viability assessment

To evaluate the effect of different treatments on DC viability, harvested mDCs were analyzed for cell viability. For each group, 20 μL of cell suspension was mixed with 20 μL of AO/PI staining solution (CS2-0106, Nexcelom) in a 1.5 mL tube. The mixture was loaded onto a disposable cell counting slide (SD100, Revvity) and analyzed using an automated cell counter (Nexcelom K2) to determine total cell density, viable cell density, and viability percentage. Each treatment was performed with at least two technical replicates.

2.7 Flow cytometry analysis

To assess DC maturation and PD-L1 expression, harvested mDCs were stained with antibodies against CD83 (305324, BioLegend), CD80 (305208, BioLegend), CD86 (305430, BioLegend), HLA-DR (307626, BioLegend), CD14 (325604, BioLegend), and PD-L1 (393606, BioLegend). For T cell activation and subset analysis, T cells collected before and after co-culture were stained with PE/Cyanine7 CD3 (300420, BioLegend), Alexa Fluor® 700 CD8 (344724, BioLegend), APC CCR7 (566762, BD Biosciences), APC/Cyanine7 CD45RA (304128, BioLegend), Brilliant Violet 421™ CD69 (310929,

BioLegend), and Brilliant Violet 605™ CXCR3 (BioLegend). Stained cells were analyzed using a BD FACS Lyric flow cytometer, and data were processed with BD FACSuite v1.4.1 and FlowJo v10.10.

2.8 ELISA for IL-12p70 secretion

The concentration of IL-12p70 in the culture supernatants, collected from mDCs following different treatment, was quantified using a human IL-12p70 ELISA kit (431704, BioLegend) following the manufacturer's instructions. Supernatants were collected and centrifuged at 500 × g for 10 min to remove cell debris, then stored at -80 °C until analysis. All samples and standards were assayed in duplicate. Plates were coated overnight (16–18 h), washed, and blocked for 1 h. After washing, samples and standards were added and incubated at room temperature for 2 h. Biotinylated detection antibody was applied for 1 h, followed by streptavidin-HRP incubation for 30 min. Color development was performed using TMB substrate, stopped with stop solution, and absorbance was measured at 450 nm with a reference wavelength of 570 nm. IL-12p70 concentrations were calculated based on the standard curve.

2.9 ELISpot assay

ELISpot was used to assess the capacity of DCs to activate T cells for IFN-γ production. Briefly, mDCs, pulsed with CMV peptide (LARNLVPMVATVQGQNLKYQE, GenScript), were co-cultured with autologous lymphocyte populations (e.g., $CD14^-$ cells) or total PBMCs at a 1:5 ratio (approximately 4×10^5 mDCs with 2×10^5 $CD14^-$/PBMC per well) in IFN-γ pre-coated 96-well plates (HU IFN-γ ELISpot Kit, CTL) for 18 h at 37 °C, 5% CO_2. After incubation, plates were washed twice with PBS and 0.05% Tween-20. Biotinylated detection antibody was added and incubated for 2 h at room temperature, followed by three washes and 30 min incubation with enzyme conjugate. After washing, substrate was added for 15 min, the reaction was stopped with distilled water, and plates were washed three times and dried. Spot numbers were analyzed using an ELISpot reader (CTL S6). Each condition was assayed in 2–3 replicate wells.

2.10 Activation of cytotoxic T-cell (CTL)

$CD8^+$ T cells were isolated from the same donor's PBMCs. After positive selection of $CD14^+$ monocytes, the remaining $CD14^-$ fraction was further enriched using $CD8^+$ nanobeads (Miltenyi Biotec). Purified $CD8^+$ T cells were co-cultured with neoantigen-loaded Neo-DCs or Mock-DCs (cultured under the same conditions without peptide) in CTL medium supplemented with immune cell serum replacement (Thermo Fisher) for 10 days, at a T cell: DC ratio of 4: 1. IL-7 (50 ng/mL, Peprotech) and IL-15 (50 ng/mL, Peprotech) were added to support T cell proliferation and survival. T cells expanded with Neo-DCs were defined as Neo-DC T, while those stimulated with Mock-DCs served as the control (Control T).

2.11 Statistical analysis

Statistical analyses for in vitro experiments were performed using GraphPad Prism software (version 8.0). Data are presented as mean ± standard deviation (SD). Comparisons among multiple groups were conducted using one-way analysis of variance (ANOVA). When variance homogeneity was met, Tukey's post hoc test was applied; otherwise,

Brown–Forsythe and Welch ANOVA followed by Dunnett's T3 multiple comparison test was used. A two-sided p value < 0.05 was considered statistically significant.

3 Results

3.1 Single-cell atlas of the LUAD tumor microenvironment

We first performed quality control on scRNA-seq data from the LUAD dataset GSE189357. After filtering low-quality cells, a total of 111,595 high-quality cells were retained for downstream analyses. Following batch effect correction, cells from the nine samples showed comparable distributions, indicating effective integration across samples (Fig. 1 A). A total of 22 distinct cell clusters were identified via UMAP (Fig. 1B). Based on differentially expressed genes (DEGs) and well-established marker genes for major LUAD cell types, these clusters were annotated into nine major cell populations, including epithelial cells, endothelial cells, T cells, natural killer (NK) cells, B cells, plasma cells, myeloid cells, mast cells, and fibroblasts (Fig. 1 C). A dotplot displaying representative marker genes further confirmed the accuracy of cell type annotation (Fig. 1D).

3.2 Construction of myeloid cell classification by single-cell transcriptomics

Given the central role of myeloid cells in shaping the tumor immune microenvironment, we next focused on the 13,404 myeloid cells identified from the global dataset. After batch correction, dimensionality reduction, and unsupervised clustering, myeloid cells were separated into 18 distinct clusters (Fig. 2A, B). Using cluster-specific DEGs and classic marker genes for LUAD-associated myeloid populations, we defined 11 myeloid

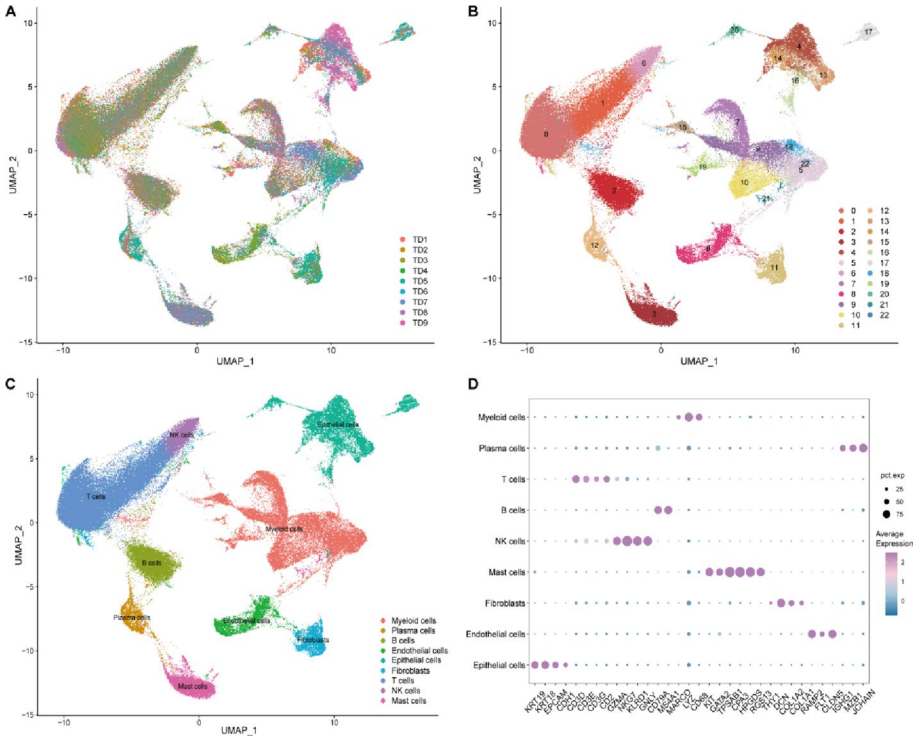

Fig. 1 Single-cell transcriptomic landscape of LUAD. **A** UMAP visualization of all cells colored by individual tumor samples after quality control and batch effect correction, showing effective integration across nine LUAD samples. **B** UMAP plot displaying unsupervised clustering of 111,595 cells into 22 distinct clusters. **C** UMAP representation of major cell populations. **D** The expression patterns of representative marker genes used for cell type annotation

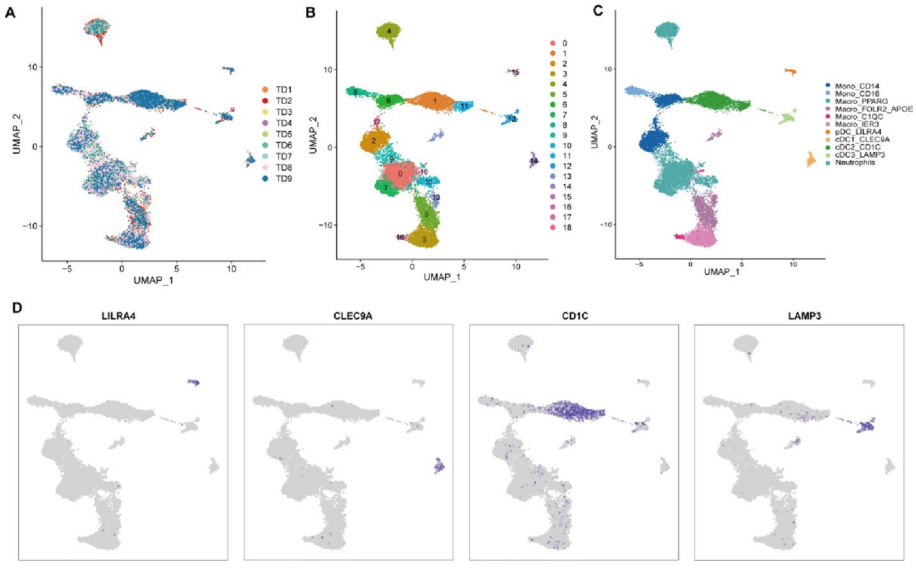

Fig. 2 Myeloid cell re-clustering reveals distinct dendritic cell subsets in LUAD. **A** UMAP visualization of myeloid cells colored by individual tumor samples after batch effect correction, showing effective integration across nine LUAD samples. **B** Unsupervised clustering of myeloid cells visualized by UMAP, identifying 18 distinct myeloid cell clusters based on transcriptional similarity. **C** UMAP plot showing annotation of myeloid cell subsets according to canonical marker genes. **D** Feature plots showing the expression of representative dendritic cell marker genes

cell subsets, including two monocyte subsets ($CD14^+$ monocytes and $CD16^+$ monocytes), four macrophage subsets ($PPARG^+$ macrophages, $FOLR2^+$/$APOE^+$ macrophages, $C1QC^+$ macrophages, and $IER3^+$ macrophages), four DC subsets (plasmacytoid DCs, conventional type 1 DCs [cDC1s], conventional type 2 DCs [cDC2s], and conventional type 3 DCs [cDC3s]), and one neutrophil subset (Neutrophils) (Fig. 2C). The expression patterns of representative DC marker genes across these clusters are shown in Fig. 2D.

Among the macrophage populations, $PPARG^+$ macrophages showed high expression of MARCO, PPARG, MRC1, MSR1, and FABP4, consistent with the transcriptional features of alveolar macrophages (AMs). AMs are the major tissue-resident macrophages (TRMs) in the lung, originating from embryonic yolk sac progenitors and maintained through self-renewal rather than continuous monocyte recruitment. These cells express multiple scavenger receptors, including SR-I, MARCO, and MerTK, enabling efficient phagocytosis and efferocytosis. AMs have been reported to contribute to the formation of an immunosuppressive microenvironment and to play an important role in LUAD progression.

Within the DC populations, we identified four transcriptionally distinct DC subsets. Previous studies have shown that cDC1s are specialized in cross-presentation and activation of $CD8^+$ T cells, whereas cDC2s primarily support $CD4^+$ T cell responses. In contrast, $LAMP3^+$ DCs (cDC3s) have been described as a population of mature DCs characterized by the expression of genes related with migration and immunoregulatory. Together, these findings indicate that DCs in LUAD are highly heterogeneous and exist in distinct functional states, providing a framework for further investigation of DC maturation and immune regulatory programs.

3.3 Transcriptional and functional heterogeneity of dendritic cell subsets in LUAD

DCs serve as a critical link between innate and adaptive immunity, playing essential roles in antigen-specific immune responses and immune tolerance. To further characterize DC-related immune regulation in LUAD, we performed an in-depth single-cell analysis focusing on DC subsets.

Cell-cell communication analysis revealed extensive interactions between DCs and other myeloid populations, particularly monocytes and macrophages. Among these interactions, cDC2s displayed strong communication with AMs, suggesting close functional coordination between these two populations within the tumor microenvironment (Fig. 3A). In addition to such interaction, substantial communication was also observed among different DC subsets. Notably, cDC1s and cDC2s exhibited strong interactions mediated by MIF-(CD74 + CXCR4) and MIF-(CD74 + CD44) ligand-receptor pairs, indicating coordinated signaling between DC subsets (Fig. 3B).

To assess functional heterogeneity among DC subsets, we compared activation- and migration-related scores across DC populations. LAMP3⁺ cDC3s showed significantly higher activation and migration scores than other DC subsets, indicating a highly activated and migratory DC state. At the molecular level, LAMP3⁺ cDC3s displayed markedly increased expression of DC maturation–related genes, including CD40, CD80, CD86, RELB, and CD83, consistent with a mature DC phenotype. In parallel, genes related to cell migration, such as CCR7, FSCN1, MARCKS, and MYO1G, were also highly expressed in this subset, further supporting their potential to migrate toward lymphoid tissues and participate in T cell priming. Despite their strong activation and maturation signatures, LAMP3⁺ cDC3s simultaneously exhibited elevated expression

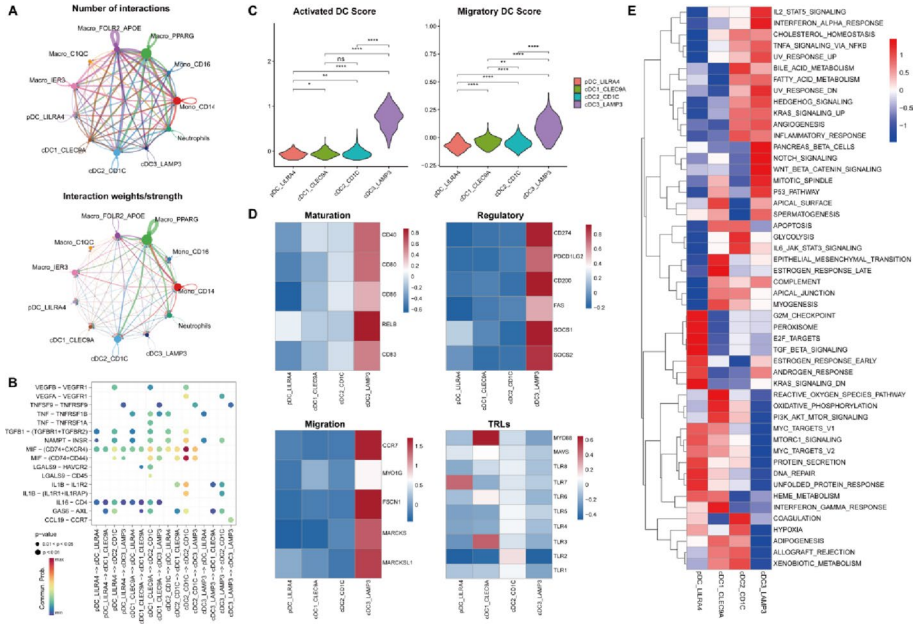

Fig. 3 Functional heterogeneity and enhanced activation potential of dendritic cell subsets. **A** CellChat-inferred intercellular communication network among myeloid cell populations, showing the number of interactions (upper) and interaction strength (lower). **B** Dot plot of representative ligand-receptor interactions involving dendritic cell subsets.**C** Violin plots comparing activation and migration scores across dendritic cell subsets. **D** Heatmaps showing scaled expression of genes associated with dendritic cell maturation, migration, immune regulation, and Toll-like receptor signaling. (E) GSVA heatmap depicting enrichment of hallmark signaling pathways across dendritic cell subsets

of multiple immunoregulatory molecules, including CD274 (PD-L1), PDCD1LG2 (PD-L2), CD200, and SOCS1/2. In contrast, the overall expression levels of Toll-like receptor (TLR) genes (TLR1-TLR9) and downstream signaling components were reduced in this subset, suggesting that LAMP3⁺ cDC3s are not in a state of continuous pathogen sensing but rather represent a post-activation DC state with built-in regulatory features.

Pathway enrichment analysis further supported this interpretation. LAMP3⁺ cDC3s were significantly enriched for pathways related to DC activation and T cell responses, including TNFα–NF-κB, IL2–STAT5, IL6–JAK–STAT3, and interferon response pathways. In addition, pathways associated with metabolic reprogramming, such as mTORC1 signaling, MYC targets, oxidative phosphorylation, and protein secretion, were upregulated in this subset. Pathways related to cell cycle regulation, DNA repair, and the unfolded protein response were also enriched, indicating increased biosynthetic and functional activity under a highly activated state.

Together, single-cell transcriptomic analyses revealed that LAMP3⁺ cDC3s represent a highly mature and migratory DC subset in LUAD. Importantly, this population exhibits strong immunostimulatory potential, while simultaneously upregulating immune checkpoint and other negative regulatory molecules. These findings suggest that DC maturation is accompanied by intrinsic immunoregulatory mechanisms, which may restrain excessive T-cell activation and influence immune responses within the tumor microenvironment.

Given the prominent expression of inhibitory molecules, particularly PD-L1, on mature DCs, we next sought to determine whether blocking PD-L1 signaling could relieve this intrinsic restraint and further enhance DC-mediated T-cell activation.

3.4 PD-L1 blockade suppresses PD-L1 expression on DCs and enhances T-cell activation

High level PD-L1 expression on DCs limits their ability to activate effective T-cell immune responses. To assess whether PD-L1 inhibition could improve DC function, we treated DCs with two different PD-L1 monoclonal antibodies (Adebrelimab and Atezolizumab) and examined their effects on surface molecule expression and functional activity. Flow cytometric analysis revealed that PD-L1 expression on DCs was significantly reduced following antibody treatment compared with the control group (Fig. 4A), indicating that both antibodies effectively downregulated PD-L1 on DC surfaces. Subsequently, an ELISpot assay was performed to evaluate the capacity of PD-L1-blocked DCs to induce T-cell responses. DCs treated with either Adebrelimab or Atezolizumab

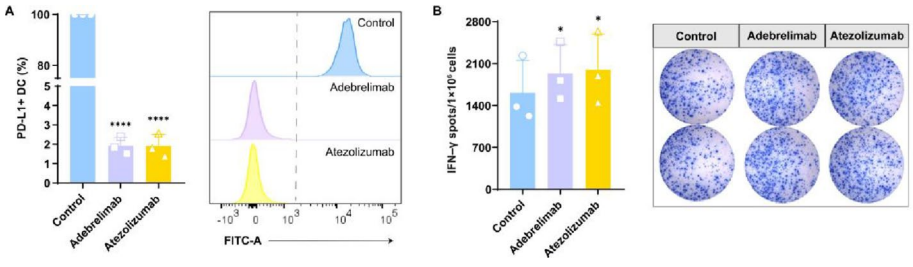

Fig. 4 PD-L1 blockade reduces DC surface PD-L1 expression and promotes T-cell activation. **A** Proportion and representative flow cytometry histograms of PD-L1⁺ DCs following treatment with Adebrelimab or Atezolizumab compared with untreated control. **B** DCs were co-cultured with autologous CD14⁻ cells, after which ELISpot assays were performed to assess T cell activation. Quantitative analysis and representative ELISpot images of IFN-γ⁺ spots in different groups were shown. Data are presented as mean ± SD (n = 3). *P < 0.05, ****P < 0.0001 vs. Control

stimulated a markedly higher number of IFN-γ⁺ T cells than untreated controls (Fig. 4B). Collectively, these findings demonstrate that blockade of PD-L1 on DCs substantially enhances their T-cell activating potential, thereby improving their overall immunostimulatory function.

3.5 CD40 agonism promote DC maturation, activation, and enhance T-cell stimulatory capacity

The CD40/CD40L axis is critical for DC activation, and CD40 agonists can effectively engage this pathway to induce DC functional activation. To comprehensively assess the potency of various CD40 activators, direct agonists (Mitazalimab, Cifurtilimab, and CD40L) and indirect stimulators (OK432 and Poly I: C) were examined for their effects on DC maturation and immunostimulatory function.

Flow cytometric analysis showed that all five CD40 agonists significantly upregulated the expression of the DC maturation marker CD83 (Fig. 5B). Notably, except for Poly I: C, none of the agents adversely affected DC viability (Fig. 5 A). Functionally, ELISA analysis demonstrated that all five CD40 agonists markedly increased IL-12p70 secretion by DCs (Fig. 5 C), indicating robust immune activation. Consistently, ELISpot assays revealed a significant elevation in the number of IFN-γ⁺ T cells induced by DCs pretreated with each of the five agonists (Fig. 5D), with Cifurtilimab showing the most pronounced effect. Collectively, these results indicate that multiple CD40 agonistic agents can enhance DC maturation and immunostimulatory capacity to varying degrees, among which Cifurtilimab exhibits the strongest immune-promoting activity.

3.6 CD40 and PD-L1 antibodies cooperatively enhance DC maturation and T-cell activation

Based on preliminary results and drug availability, Atezolizumab and Cifurtilimab were selected for combination treatment to assess their synergistic potential in promoting DC activation. Compared with PD-L1 antibody treatment alone, the combination significantly upregulated the expression of the maturation marker CD83 on DCs while

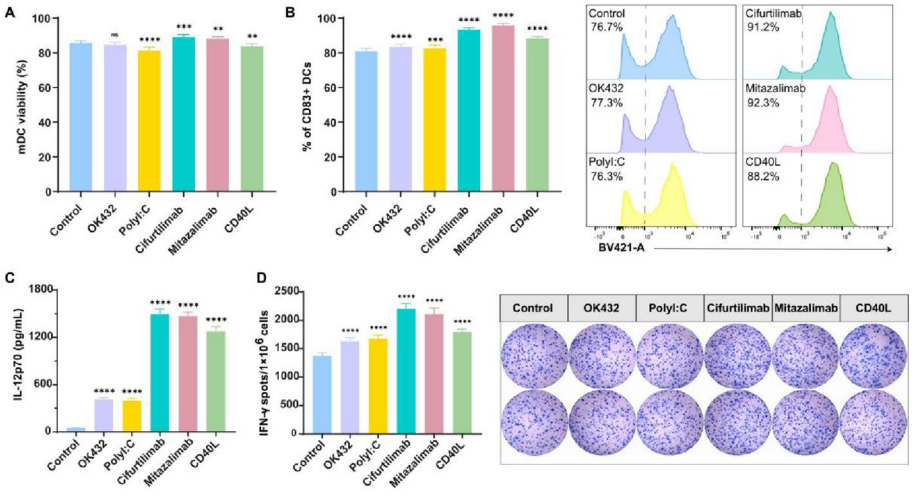

Fig. 5 Effects of different CD40 agonistic agents on DC maturation and activation. **A** Viability of mDC following treatment with different CD40 antibodies or untreated. **B** Proportion of CD83⁺ DCs and representative flow cytometry histograms in different groups, with representative flow cytometry histograms. **C** IL-12p70 secretion of DC in different groups. **D** DCs treated as indicated were co-cultured with autologous CD14⁻ cells, followed by ELISpot assays to assess T-cell activation. Quantitative analysis and representative images of IFN-γ⁺ spots are shown. Data are presented as mean ± SD (n = 3). *P < 0.05,***P < 0.001, ****P < 0.0001 vs. Control

maintaining cell viability (Fig. 6A, B). Functionally, the combination further potentiated DC activation, as evidenced by a marked increase in IL-12p70 secretion compared with PD-L1 antibody alone (Fig. 6C). Although ELISpot analysis revealed only a trend toward higher frequencies of IFN-γ⁺ T cells in the combination group relative to PD-L1 mono-treated group ($p = 0.09$, Fig. 6D), a statistically significant increase in IFN-γ⁺ T-cell induction was observed when compared with the untreated control ($p < 0.0001$) (Fig. 6E). Notably, this enhancement was observed specifically under peptide-pulsed conditions (Fig. 6E), suggesting that the combined treatment reinforced antigen presentation and promoted antigen-dependent T-cell activation by DCs. Collectively, these results demonstrate that dual targeting of CD40 and PD-L1 cooperatively enhances DC maturation, activation, and T-cell stimulatory function. Accordingly, we define these cells as "Enhanced DCs", which were subsequently applied for neoantigen loading and evaluation of anti-tumor immune responses.

3.7 Neoantigen-loaded enhanced DCs promote CD8⁺ T-cell activation and memory differentiation in vitro

To evaluate the potential of Enhanced DCs in a neoantigen vaccine strategy, Enhanced DCs were loaded with synthetic peptides derived from the neoantigen $p53^{R175H}$ to generate a neoantigen-loaded DC vaccine (Neo-DC).

Neo-DCs and Mock-DCs (without neoantigen loaded) were co-cultured with T cells to generate Neo-DC T and Control T populations, respectively. Flow cytometric

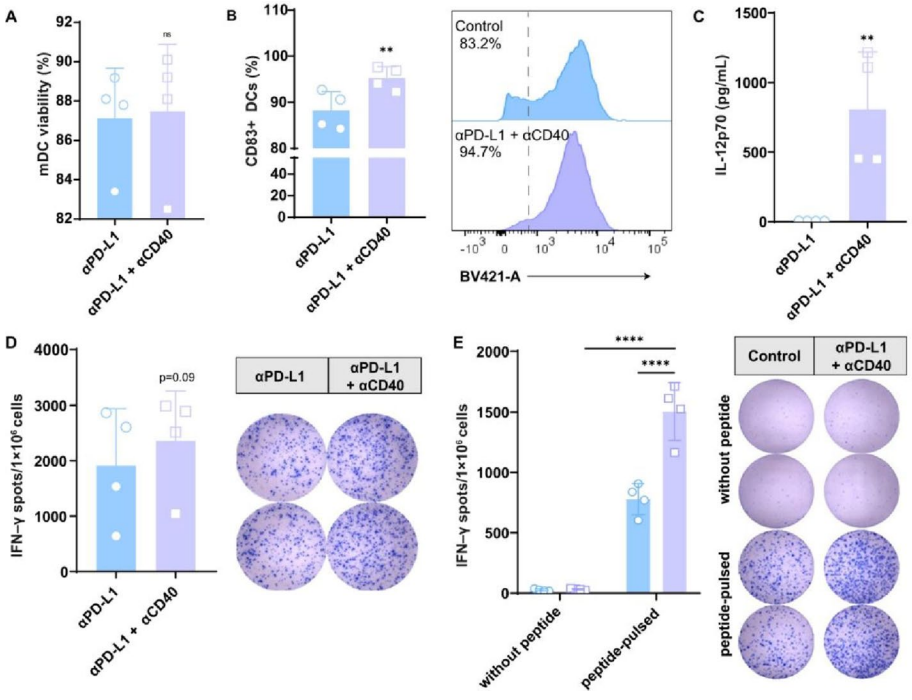

Fig. 6 Combination of anti-PD-L1 and CD40 agonist enhanced DC maturation and function. **A** Viability of mDCs treated with PD-L1 antibody alone or in combination with CD40 antibody. **B** Proportion of CD83⁺ DCs and representative flow cytometry histograms in the two groups. **C** IL-12p70 secretion levels of DCs following different treatments. **D** DCs were co-cultured with autologous CD14⁻ cells, and T-cell activation was evaluated by ELISpot assay showing IFN-γ⁺ spot quantification and representative images. **E** DCs, either peptide-pulsed or unpulsed, were treated with the combination of anti-PD-L1 antibody and CD40 agonist or left untreated, and then co-cultured with autologous CD14⁻ T cells. T-cell activation was evaluated by IFN-γ ELISpot assay, with quantified spot numbers and representative images shown. Data are presented as mean ± SD (n = 4). *P< 0.05, **P < 0.01, ****P < 0.0001

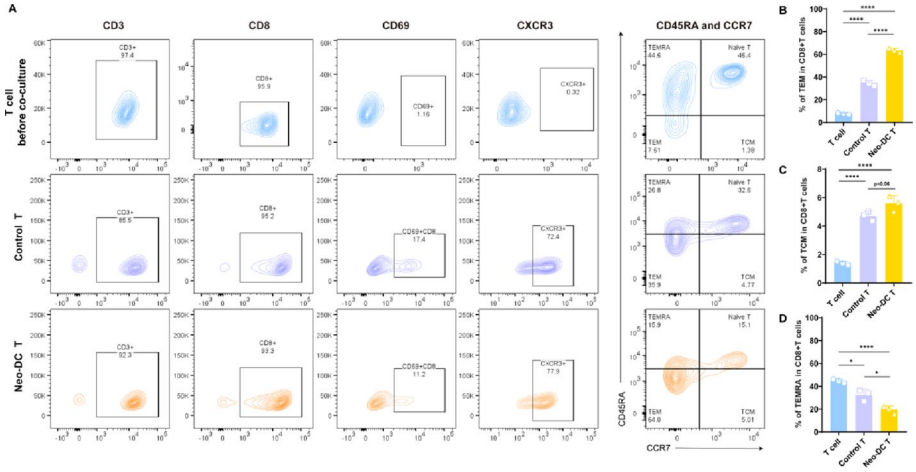

Fig. 7 Neoantigen-loaded enhanced DCs promote CD8⁺ T-cell activation and neoantigen-specific tumor cell killing in vitro.**A** Flow cytometry profiles of CD8⁺ T cells before stimulation, Control T cells induced by Mock-DCs, and Neo-DC T cells stimulated with Neo-DC. Cells were stained with specific antibodies, and the proportions of positive subsets were analyzed. **B**–**D**, Subset analysis of TEM (**B**), TCM (**C**), and TEMRA (**D**) among the three T-cell groups. Data are presented as mean ± SD (n= 3). ns, not significant, *P < 0.05, **P < 0.01, ***P < 0.001, ****P< 0.0001

analysis revealed that the proportions of CD69⁺ and CXCR3⁺ CD8⁺ T cells were significantly increased in both Neo-DC T and Control T compared with baseline (Fig. 7A–C), indicating effective T-cell activation by both DC populations. Memory phenotype analysis of CD8⁺ T cells, based on CCR7 and CD45RA expression, categorized cells into four major subsets: naïve T cells (CCR7⁺CD45RA⁺), central memory T cells (TCM, CCR7⁺CD45RA⁻), effector memory T cells (TEM, CCR7⁻CD45RA⁻), and terminally differentiated effector memory T cells (TEMRA, CCR7⁻CD45RA⁺). Compared with pre-culture T cells, both Neo-DC T and Control T showed significant increases in TCM and TEM subsets. Notably, the average proportions of TEM and TCM in Neo-DC T were 1.8-fold and 1.2-fold higher, respectively, than those in Control T (Fig. 7A–C). Conversely, the TEMRA subset was significantly reduced in Neo-DC T compared with both pre-culture and Control T (Fig. 7A, D). These data suggest that Neo-DCs induce T-cell responses toward memory subsets with higher proliferative potential and sustained functionality, which may enhance overall T-cell quality and long-term immune surveillance.

4 Discussion

In this study, we systematically evaluated the effects of PD-L1 and CD40 antibodies on DC maturation and functional enhancement and further explored the potential value of their combined application in neoantigen-loaded DC vaccines. By integrating single-cell transcriptomic analysis with functional validation experiments, our study provides a coherent framework linking DC functional states observed in tumors with strategies to optimize DC activity ex vivo.

Our single-cell RNA sequencing analysis revealed substantial heterogeneity among DC subsets in lung adenocarcinoma, with LAMP3⁺ cDC3s representing a highly mature and migratory DC state. Notably, this subset displayed concurrent upregulation of antigen presentation, co-stimulatory, and migration-related genes, together with increased expression of immune regulatory molecules such as PD-L1 and PD-L2. These findings suggest that DC maturation in the tumor microenvironment is accompanied by intrinsic

immune regulatory mechanisms, potentially limiting excessive T cell activation. This observation provided a mechanistic rationale for targeting immune checkpoint signaling and co-stimulatory pathways to functionally enhance DCs.

Previous studies have shown that PD-L1 is widely expressed on DCs, macrophages, and other APCs, and can be upregulated by IFN-γ in the tumor microenvironment, thereby suppressing T-cell activation via the PD-1/PD-L1 pathway and impairing anti-tumor immunity [17–21]. Consistent with these studies, we found that blocking PD-L1 on DCs effectively relieved immune inhibitory signaling and enhanced their capacity to activate T cells. Treatment with different PD-L1 antibodies, including Adbrelimab and Atezolizumab, reduced surface PD-L1 expression on DCs and increased their ability to induce IFN-γ^+ T-cell activation. These findings are in agreement with previous reports indicating that PD-L1 inhibition can restore DC immune-stimulatory function and enhance their potential as vaccine adjuvants [10, 11, 21, 22].

In parallel, activation of the CD40/CD40L signaling axis markedly promoted DC maturation and functional activation [23, 24]. In our study, five different agonistic agents not only upregulated DC CD83 expression and IL-12p70 secretion but also enhanced T-cell activation, among which Cifurtilimab exhibiting the most pronounced effect. These findings are consistent with previous preclinical studies showing that CD40 agonists can enhance DC maturation and activation and promote antigen-specific T-cell responses, establishing CD40 as a promising target for cancer immunotherapy [12, 25, 26]. Importantly, our results further demonstrate that the combination of CD40 and PD-L1 antibodies significantly enhances DC function while preserving cell viability. The underlying mechanism likely involves dual signaling: PD-L1 blockade relieves immunosuppression, while CD40 stimulation drives DCs to full maturation and activation, collectively leading to enhanced T-cell effector function. Supporting this, in vivo studies have shown that CD40 activation combined with PD-1/PD-L1 blockade can overcome resistance to anti-PD-1 therapy, improving immunotherapeutic outcomes [27–29].

Given the central role of DCs in antigen processing and presentation, we further evaluated whether Enhanced DCs could improve neoantigen-specific T cell responses. Enhanced DCs were subsequently loaded with neoantigen peptides (Neo-DCs) and significantly induced stronger $CD8^+$ T cell activation in vitro compared with control DCs. More importantly, Neo-DCs promoted the differentiation of $CD8^+$ T cells toward memory-associated phenotypes, including central memory (TCM) and effector memory (TEM) subsets. These findings are consistent with growing clinical evidence indicating that durable antitumor immunity depends not only on immediate effector responses but also on the generation of long-lived memory T cells [30, 31].

Nevertheless, several limitations of this study should be acknowledged. First, the DCs used in functional assays were derived from peripheral blood monocytes and may not fully recapitulate all transcriptional features of tumor-infiltrating DC subsets identified by single-cell analysis. Second, our study mainly focused on PD-L1 and CD40 pathways, future studies could explore combinations with other immune pathways (e.g., STING, TLRs, or OX40) to further optimize DC vaccine efficacy. Finally, the safety, durability, and clinical translatability of Neo-DC vaccines require additional preclinical and clinical validation.

5 Conclusion

In summary, by integrating single-cell transcriptomic profiling with functional experiments, our study demonstrates that PD-L1 blockade combined with CD40 activation effectively enhances dendritic cell maturation, activation, and T cell-stimulating capacity. Neoantigen-loaded Enhanced DCs robustly activate $CD8^+$ T cells and promote their differentiation into effector and memory subsets. These findings provide a mechanistic basis for rational DC functional optimization and highlight a promising strategy to improve neoantigen-directed immunotherapy.

Author contributions

Li Y and Li H contributed equally to this work. Li Y, Cheng X and Xu J contributed conception and design of the study. Li Y and Li C performed single-cell RNA sequencing data analysis and interpretation. Li Y, Li H, Ma X and Cheng X conducted in vitro experiments. Li Y, Liu R, Ye S and Li J performed the statistical analysis; Li Y and Li H wrote the first draft of the manuscript; Cheng X and Xu J revised the manuscript. All authors reviewed and approved the final manuscript.

Data availability

The single-cell RNA sequencing data analyzed in this study were obtained from the publicly available Gene Expression Omnibus (GEO) database under accession number GSE189357.

Declarations

Competing interests

The authors declare no competing interests.

Received: 23 January 2026 / Accepted: 9 March 2026
Published online: 13 March 2026

References

1. Wculek SK, Cueto FJ, Mujal AM, Melero I, Krummel MF, Sancho D. Dendritic cells in cancer immunology and immunotherapy. Nat Rev Immunol. 2020;20:7–24. https://doi.org/10.1038/s41577-019-0210-z.
2. Wang Y, Xiang Y, Xin VW, Wang X-W, Peng X-C, Liu X-Q, et al. Dendritic cell biology and its role in tumor immunotherapy. J Hematol Oncol. 2020;13:107. https://doi.org/10.1186/s13045-020-00939-6.
3. Sellars MC, Wu CJ, Fritsch EF. Cancer vaccines: building a bridge over troubled waters. Cell. 2022;185:2770–88. https://doi.org/10.1016/j.cell.2022.06.035.
4. Liu J, Fu M, Wang M, Wan D, Wei Y, Wei X. Cancer vaccines as promising immuno-therapeutics: platforms and current progress. J Hematol Oncol. 2022;15:28. https://doi.org/10.1186/s13045-022-01247-x.
5. Harari A, Graciotti M, Bassani-Sternberg M, Kandalaft LE. Antitumour dendritic cell vaccination in a priming and boosting approach. Nat Rev Drug Discov. 2020;19:635–52. https://doi.org/10.1038/s41573-020-0074-8.
6. Saxena M, Bhardwaj N. Turbocharging vaccines: emerging adjuvants for dendritic cell based therapeutic cancer vaccines. Curr Opin Immunol. 2017;47:35–43. https://doi.org/10.1016/j.coi.2017.06.003.
7. Datsi A, Sorg RV. Dendritic cell vaccination of glioblastoma: road to success or dead end. Front Immunol. 2021;12:770390. https://doi.org/10.3389/fimmu.2021.770390.
8. Braun DA, Moranzoni G, Chea V, McGregor BA, Blass E, Tu CR, et al. A neoantigen vaccine generates antitumour immunity in renal cell carcinoma. Nature. 2025;639:474–82. https://doi.org/10.1038/s41586-024-08507-5.
9. Ott PA, Hu Z, Keskin DB, Shukla SA, Sun J, Bozym DJ, et al. An Immunogenic Personal Neoantigen Vaccine for Melanoma Patients. Nature. 2017;547:217–21. https://doi.org/10.1038/nature22991.
10. M M, A R, V P, S S, S C, E S, et al. Dendritic cells dictate responses to PD-L1 blockade cancer immunotherapy. Sci Transl Med. 2020. https://doi.org/10.1126/scitranslmed.aav7431.
11. Curiel TJ, Wei S, Dong H, Alvarez X, Cheng P, Mottram P, et al. Blockade of B7-H1 improves myeloid dendritic cell–mediated antitumor immunity. Nat Med. 2003;9:562–7. https://doi.org/10.1038/nm863.
12. Vonderheide RH. CD40 agonist antibodies in cancer immunotherapy. Annu Rev Med. 2020;71:47–58. https://doi.org/10.1146/annurev-med-062518-045435.
13. Van Kooten C, Banchereau J. CD40-CD40 ligand. J Leukoc Biol. 2000;67:2–17. https://doi.org/10.1002/jlb.67.1.2.
14. Sa O, Dc W, J C, A N, H X, R C, et al. PD-L1 expression by dendritic cells is a key regulator of T-cell immunity in cancer. Nature cancer. 2020. https://doi.org/10.1038/s43018-020-0075-x.
15. Pearlman AH, Hwang MS, Konig MF, Hsiue E-C, Douglass J, DiNapoli SR, et al. Targeting public neoantigens for cancer immunotherapy. Nat Cancer. 2021;2:487–97. https://doi.org/10.1038/s43018-021-00210-y.
16. Hsiue E-C, Wright KM, Douglass J, Hwang MS, Mog BJ, Pearlman AH, et al. Targeting a neoantigen derived from a common TP53 mutation. Science. 2021;371:eabc8697. https://doi.org/10.1126/science.abc8697.
17. Q P, X Q, Z Z, S Z, Y Z, Y L, et al. PD-L1 on dendritic cells attenuates T cell activation and regulates response to immune checkpoint blockade. Nat Commun. 2020. https://doi.org/10.1038/s41467-020-18570-x.
18. Tang H, Liang Y, Anders RA, Taube JM, Qiu X, Mulgaonkar A, et al. PD-L1 on host cells is essential for PD-L1 blockade-mediated tumor regression. J Clin Invest. 2018;128:580–8. https://doi.org/10.1172/JCI96061.
19. Francisco LM, Sage PT, Sharpe AH. The PD-1 pathway in tolerance and autoimmunity. Immunol Rev. 2010;236:219–42. https://doi.org/10.1111/j.1600-065X.2010.00923.x.

20. Xiao K, Zhang S, Peng Q, Du Y, Yao X, Ng I-I, et al. PD-L1 protects tumor-associated dendritic cells from ferroptosis during immunogenic chemotherapy. Cell Rep. 2024;43:114868. https://doi.org/10.1016/j.celrep.2024.114868.
21. Sun N-Y, Chen Y-L, Wu W-Y, Lin H-W, Chiang Y-C, Chang C-F, et al. Blockade of PD-L1 enhances cancer immunotherapy by regulating dendritic cell maturation and macrophage polarization. Cancers (Basel). 2019;11:1400. https://doi.org/10.3390/cancers11091400.
22. Pilon-Thomas S, Mackay A, Vohra N, Mulé JJ. Blockade of PD-L1 enhances the therapeutic efficacy of combination immunotherapy against melanoma. J Immunol. 2010;184:3442–9. https://doi.org/10.4049/jimmunol.0904114.
23. Lanzavecchia A. Immunology. Licence to kill. Nature. 1998;393:413–4. https://doi.org/10.1038/30845.
24. Vonderheide RH. Prospect of targeting the CD40 pathway for cancer therapy. Clin Cancer Res. 2007;13:1083–8. https://doi.org/10.1158/1078-0432.CCR-06-1893.
25. Lau SP, Montfoort N, Kinderman P, Lukkes M, Klaase L, Nimwegen M, et al. Dendritic cell vaccination and CD40-agonist combination therapy licenses T cell-dependent antitumor immunity in a pancreatic carcinoma murine model. J Immunother Cancer. 2020;8:e000772. https://doi.org/10.1136/jitc-2020-000772.
26. Byrne KT, Vonderheide RH. CD40 stimulation obviates innate sensors and drives T cell immunity in cancer. Cell Rep. 2016;15:2719–32. https://doi.org/10.1016/j.celrep.2016.05.058.
27. Zippelius A, Schreiner J, Herzig P, Müller P. Induced PD-L1 expression mediates acquired resistance to agonistic anti-CD40 treatment. Cancer Immunol Res. 2015;3:236–44. https://doi.org/10.1158/2326-6066.CIR-14-0226.
28. Ngiow SF, Young A, Blake SJ, Hill GR, Yagita H, Teng MWL, et al. Agonistic CD40 mAb-driven IL12 reverses resistance to anti-PD1 in a T-cell-rich tumor. Cancer Res. 2016;76:6266–77. https://doi.org/10.1158/0008-5472.CAN-16-2141.
29. Diggs LP, Ruf B, Ma C, Heinrich B, Cui L, Zhang Q, et al. CD40-mediated immune cell activation enhances response to anti-PD-1 in murine intrahepatic cholangiocarcinoma. J Hepatol. 2021;74:1145–54. https://doi.org/10.1016/j.jhep.2020.11.037.
30. Bobisse S, Bianchi V, Tanyi JL, Sarivalasis A, Missiaglia E, Pétremand R, et al. A phase 1 trial of adoptive transfer of vaccine-primed autologous circulating T cells in ovarian cancer. Nat Cancer. 2023;4:1410–7. https://doi.org/10.1038/s43018-023-00623-x.
31. Ding Z, Li Q, Zhang R, Xie L, Shu Y, Gao S, et al. Personalized neoantigen pulsed dendritic cell vaccine for advanced lung cancer. Signal Transduct Target Ther. 2021;6:26. https://doi.org/10.1038/s41392-020-00448-5.

Publisher's Note